ChemPubSoc Europe

DOI: 10.1002/chem.201403042

CHEMISTRY A European Journal Communication

Single-Ion Magnets

The Metallofullerene Field-Induced Single-Ion Magnet $HoSc_2N@C_{80}$

Jan Dreiser,*[a] Rasmus Westerström,[b] Yang Zhang,[c] Alexey A. Popov,[c] Lothar Dunsch,[c] Karl Krämer,[d] Shi-Xia Liu,[d] Silvio Decurtins,[d] and Thomas Greber*[e]

Abstract: The low-temperature magnetic properties of the endohedral metallofullerene $HoSc_2N@C_{80}$ have been studied by superconducting quantum interference device (SQUID) magnetometry. Alternating current (ac) susceptibility measurements reveal that this molecule exhibits slow relaxation of magnetization in a small applied field with timescales in the order of milliseconds. The equilibrium magnetic properties of $HoSc_2N@C_{80}$ indicate strong magnetic anisotropy. The large differences in magnetization relaxation times between the present compound and the previously investigated $DySc_2N@C_{80}$ are discussed.

Lanthanides have a long-standing tradition in magnetism owing to their large and often anisotropic magnetic moments. Currently, these properties boost the synthesis of new single-molecule magnets[1] (SMMs) and single-ion magnets (SIMs), that is, SMMs containing only a single magnetic ion.[2] Most SMMs known to date are synthesized within the field of coordination chemistry. Only recently it was discovered that also the endohedral metallofullerenes (EMFs) $DySc_2N@C_{80}$ (**1**),[3] $Dy_2ScN@C_{80}$, and $Dy_3N@C_{80}$ containing one to three magnetic ions exhibit SMM behavior.[4] Such EMFs represent truly molecular systems, where a small and otherwise unstable metal nitride cluster is incorporated in a C_{80} cage.[5] In the nitride clusterfullerenes, metal atoms (Sc, Y, or a lanthanide) adopt a trivalent state, the formal charge of the central nitride ion is −3, and the carbon cage has a formal net charge of −6. The $M_3N@C_{80}$ molecules are therefore diamagnetic, unless the encapsulated lanthanide ions have a partially filled 4f shell, which is then the only source of paramagnetism in such molecules.[5d] Thus, the exceptional properties of $DySc_2N@C_{80}$, such as its hour-long relaxation time at 2 K, can be explained by a strong easy-axis type magnetic anisotropy[6] introduced by the Dy–N bond as well as by the protective role of the cage which does not carry a magnetic moment by itself. Almost all trivalent lanthanide ions can be entrapped with different stoichiometries in this particular type of EMFs, opening a vast field of structurally closely related magnetic compounds.[5] It is particularly interesting to study the magnetic properties of the Ho member of the monolanthanide $LnSc_2N@C_{80}$ series and compare it to **1** because of its equally strong magnetic moment while it exhibits an integer total angular momentum J as compared to half integer in **1**. Also, the natural abundance of Ho is limited to a single isotope with nuclear spin $I=7/2$, which makes $HoSc_2N@C_{80}$[7] (**2**) an interesting model system to study magnetization dynamics.

Herein we show by superconducting quantum interference device (SQUID) magnetometry that **2** displays SMM behavior, albeit on a shorter time scale than in **1**. We report its equilibrium magnetic properties and magnetization lifetimes in the order of milliseconds. Field-dependent magnetization measurements obtained at low temperatures on drop-cast samples of **2** reveal strong magnetic anisotropy of the Ho^{III} ion. The alternating current (ac) susceptibility data exhibit frequency-dependent peaks that shift with temperature, indicating thermally activated relaxation of the Ho magnetic moment.

The structure of **2** obtained from geometry optimization using density-functional theory (DFT) is shown in Figure 1. The endohedral $HoSc_2N$ unit is almost trigonal planar with a Ho–N bond length of 2.163 Å and the shortest Ho–C distance of 2.405 Å. The barrier for the rotation of the nitride clusters within the C_{80}-I_h cage has been calculated to be below 100 meV.[8]

The field-dependent magnetization and the reduced magnetization are shown in Figure 2 along with the χT product, with χ representing the magnetic susceptibility. At the lowest temperatures, the magnetization reaches saturation already at fields of about 20 kOe, indicating the presence of a sizeable magnetic moment. The observed reduced magnetization

[a] Dr. J. Dreiser
Institute of Condensed Matter Physics
Ecole Polytechnique Fédérale de Lausanne
1015 Lausanne (Switzerland)
and
Swiss Light Source, Paul Scherrer Institut
5232 Villigen PSI (Switzerland)
E-mail: jan.dreiser@epfl.ch

[b] Dr. R. Westerström
Physik-Institut, Universität Zürich, 8057 Zürich (Switzerland)
and
Swiss Light Source, Paul Scherrer Institut
5232 Villigen PSI (Switzerland)
and
Department of Physics and Astronomy, Uppsala University
751 20 Uppsala (Sweden)

[c] Dr. Y. Zhang, Dr. A. A. Popov, Prof. L. Dunsch
Department of Electrochemistry and Conducting Polymers, Leibniz Institute of Solid State and Materials Research, 01069 Dresden (Germany)

[d] Dr. K. Krämer, Dr. S.-X. Liu, Prof. S. Decurtins
Departement für Chemie und Biochemie, Universität Bern
3012 Bern (Switzerland)

[e] Prof. T. Greber
Physik-Institut, Universität Zürich, 8057 Zürich (Switzerland)
E-mail: greber@physik.uzh.ch

Supporting information for this article is available on the WWW under http://dx.doi.org/10.1002/chem.201403042.

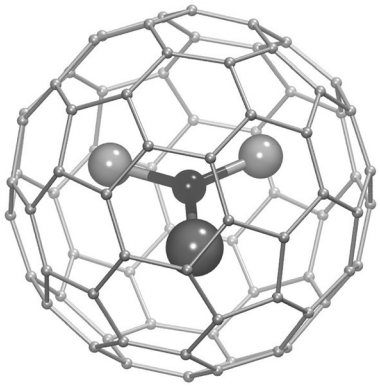

Figure 1. Structure of **2** as obtained from DFT. The C_{80} cage and the endohedral $HoSc_2N$ unit are shown as small and large spheres, respectively, with the Ho atom pointing towards the reader.

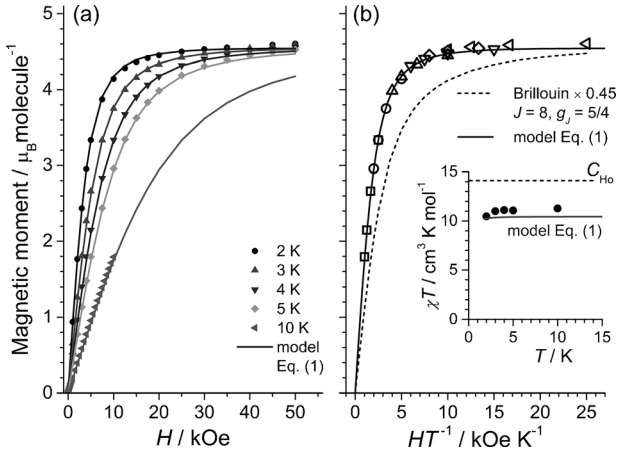

Figure 2. a) Field-dependent magnetization of **2**. Data and best-fit curves are shown as symbols and solid lines, respectively. b) Reduced magnetization of **2**. The solid and dashed lines are calculated curves obtained from model Eq. (1) and the scaled Brillouin function for $J=8$ and $g_J=5/4$. The low-temperature χT product is shown in the inset. Note that the random orientation of the Ho–N bonds reduces the saturation magnetization by a factor of two compared to the free ion.

strongly deviates from the Brillouin function calculated for Ho^{III} with its $^5I_8$ ground state and its total angular momentum of $J=8$. Moreover, the low-temperature χT product has an approximately constant value of about 11 $cm^3 K mol^{-1}$, which is lower than the calculated value of 14.1 $cm^3 K mol^{-1}$ for an isotropic paramagnet of $J=8$ and the Landé g-factor $g_J=5/4$ as obtained from the Curie law. These observations clearly demonstrate the presence of strong magnetic anisotropy. To obtain quantitative insight, we fitted the magnetic behavior of the Ho^{III} ion with a pseudospin $\sigma=1/2$ approach,[9] which considers the lowest energy quasi-doublet. In this effective-Hamiltonian formalism, the magnetic anisotropy induced by the strong ligand field of the central nitride ion appears in the diagonal, anisotropic **g**-tensor with longitudinal g-factor g_{zz}, taking the z-axis oriented parallel to the main symmetry axis. In the case of isolated doublets, according to Griffith's theorem,[7,10] $g_{xx}=g_{yy}=0$. Although no strict degeneracy of the Ho^{III} energy levels needs to be present, we assume quasi-degenerate doublets split from one another owing to the ligand field (see discussion below). A small intra-doublet splitting is neglected to avoid over-parameterization of the model. With these conditions, the Hamiltonian reads:

$$\hat{H} = \mu_B \mu_0 \hat{\sigma}_z \cdot g_{zz} \cdot H_z \qquad (1)$$

with $\hat{\sigma}_z$ the z component of the pseudospin-1/2 operator, g as mentioned before, and H_z the magnetic field component along the z direction. The field- and temperature-dependent magnetization is then given by $M = -g_{zz} \cdot \langle \hat{\sigma}_z \rangle$, in which the brackets denote the quantum-mechanical expectation value. As both the C_{80} cage and its endohedral unit are frozen, that is, rotations are unlikely at the temperatures of our experiments, a directional ("powder") average was performed.[11] Least-squares fitting of the 2 K magnetization data with this model yields $g_{zz}=18.3(1)$, corresponding to a magnetic moment of 9.15 μ_B, which is close to the maximum value of 10 μ_B for Ho^{III}. From the fits we also obtain a sample mass of 0.91 mg, which compares well with the used amount of sample. The best-fit curves are shown as solid lines in Figure 2a, demonstrating excellent agreement with the experimental data. Small deviations in the susceptibility and the high-field magnetization are probably due to imperfections in the background subtraction and second-order effects, respectively. The latter lead to admixture of excited doublets at large magnetic fields, giving rise to a small slope in the saturation regime. The value found for g_{zz} corresponds to a ground state characterized by[12] $m_{J,GS}=g_{zz}/(2\,g_J)=7.4$, and thus it is close to the largest possible $m_J=\pm 8$ allowed for $J=8$.

The out-of-phase component of the ac susceptibility of **2** measured at a constant dc field of $H_{dc}=2$ kOe is plotted in Figure 3. A shift of the peak frequency towards larger values with increasing temperature indicates a thermally activated re-

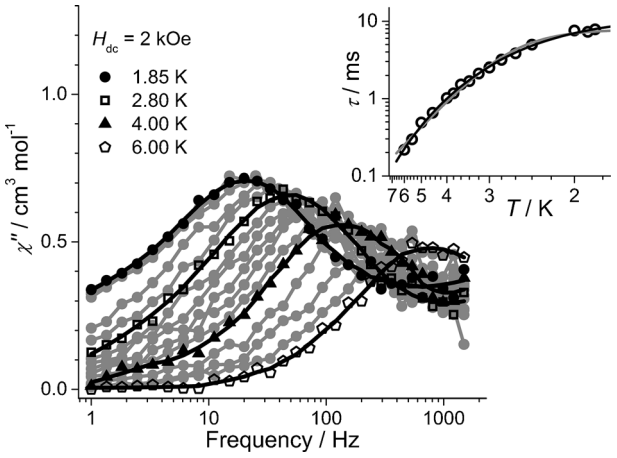

Figure 3. Out-of-phase component of the ac magnetic susceptibility of **2** as a function of frequency of the oscillating field and temperature. Data points are shown as full circles and solid lines are guides to the eyes. The Arrhenius plot is shown in the inset. Data are shown as open circles and solid lines denote best-fit curves obtained using Equations (2) (gray) and (3) (black). Error bars are smaller than the symbols.

laxation of magnetization. This is strongly supported by the simultaneous decrease of the in-phase signal towards high frequencies (compare with Figure S2 in the Supporting Information). The relaxation times obtained by fitting an extended Casimir–Du Pré model[13] to the ac susceptibility data are shown as an Arrhenius plot in the inset of Figure 3. The curve flattens towards low temperatures, which is likely to be due to the existence of different mechanisms for magnetization relaxation, each of them dominant in different temperature ranges. Fitting the data with an effective barrier Δ_{eff} for magnetization reversal like that of an Orbach process, and temperature-independent quantum tunneling of magnetization (QTM):

$$\tau^{-1} = \tau_0^{-1} \exp(-\Delta_{eff}/k_B T) + \tau_{QTM}^{-1} \quad (2)$$

as used for **1**[3] yields good agreement. The best-fit parameters are $\tau_{QTM} = 7.8(5)$ ms, $\Delta_{eff}/k_B = 16.5(6)$ K, and $\tau_0 = 1.7(2) \times 10^{-5}$ s. The barrier Δ_{eff} is of the same order of magnitude as that found for **1**,[3] and its size is much larger than the Zeeman splitting between the ground states of about 2.5 K at $H =$ 2 kOe. However, better agreement can be achieved by fitting another three-parameter model, such as:

$$\tau^{-1} = CT^n + \tau_{QTM}^{-1} \quad (3)$$

It takes into account temperature-dependent two-phonon Raman processes[2l,m,14,15] ($n \geq 4$) in the first term and QTM. Best-fit parameters are $C = 4(1)\ s^{-1} K^{-n}$, $n = 3.9(2)$, and $\tau_{QTM} =$ 13(2) ms. The standard deviation of the ratios between the calculated values from this model [Equation (3)] and the experimental data shown in the inset of Figure 3 is as low as 4%, while that obtained from the model Equation (2) is 9%. Also, the attempt time τ_0 found here is significantly longer than in conventional lanthanide SMMs and SIMs, in which τ_0 is typically found to be in the 10^{-9}–10^{-7} s range. Furthermore, an estimation of the separation between the magnetic ground states and the first excited states using point-charge model calculations[16,17] yields several hundreds of wavenumbers, which is far higher than the effective barrier Δ_{eff}. While an Orbach mechanism as in Equation (2) requires the presence of magnetic states separated from the ground states by the energy of the effective barrier Δ_{eff}, this is not the case for the two-phonon Raman mechanism. Thus the model in Equation (3) seems to be the more appropriate description in this case, and it might also reconcile data and theory in the case of **1**.[3] The best-fit value of τ_{QTM} is well within the typical range for SMMs and SIMs, whereas the value of $C = 4\ s^{-1} K^{-1}$ of the two-phonon Raman process is about one order of magnitude larger than in, for example, Er(trensal) with $C = 0.17\ s^{-1} K^{-8}$ as observed previously.[2l] It is also larger than the values of $C = 10^{-3}$–$0.47\ s^{-1} K^{-5}$ in a series of Fe^{II} SIMs.[15] In the latter, exponents of $n = 4$–5 were found, and for Er(trensal) $n = 8$. An extensive comparison of these parameters with other SMMs and SIMs is precluded because only very few studies so far have quantitatively addressed the issue of non-Arrhenius relaxation in SMMs or SIMs.

An examination of the field dependence of the out-of-phase magnetic susceptibility χ'' (see Figure S1 in the Supporting Information) reveals that at small fields of up to $H_{dc} = 1$ kOe, a fast mechanism with peak frequency beyond the measurement range of our instrument ($f_{fast} > 1.5$ kHz) dominates, while a further increase of the dc field leads to the appearance of the slow process ($f_{slow} \approx 25$ Hz), the temperature dependence of which was discussed above. The deceleration of the magnetization relaxation upon application of a magnetic field corroborates that the dominant relaxation mechanism at the lowest fields and temperatures used in this work is indeed QTM. Since QTM is temperature-independent, the two-phonon Raman process dominates at elevated temperatures larger than $T \approx 3$ K. The direct relaxation process involving a phonon resonant with the Zeeman splitting of about 2.5 K at $H =$ 2 kOe, which is in principle expected to be present[9] is not needed to reproduce the data as shown in Figure 3. Nevertheless, it may still have some influence, as it typically limits the magnetization relaxation times at large magnetic fields.[2l,m,15] Also, neglecting it in Equation (3) could be the reason for the low value of the exponent n, which for the two-phonon process was initially predicted to be $n = 7$ for non-Kramers ions.[9]

It is highly remarkable that the magnetization of **1** is retained more than five orders of magnitude longer than in **2** at the same temperatures and magnetic fields. While in both **1** and **2** the ligand field lifts the degeneracy of the ground-state multiplets, there are fundamental differences between Dy^{III} and Ho^{III} ions: The former is an odd-electron (Kramers) system, and the latter has an even number of electrons. Kramers theorem, which applies to odd-electron systems, imposes that the degeneracy of the Dy^{III} states cannot be fully lifted but, disregarding the symmetry of the ligand field, a double degeneracy has to remain in the absence of magnetic fields. In real systems, this degeneracy is eventually lifted by intermolecular and hyperfine magnetic fields, thus enabling the presence of a small tunnel splitting proportional to the perpendicular effective g-factors g_{xx} and g_{yy} of the lowest Kramers doublet.[6,18] In first-order perturbation theory, g_{xx} and g_{yy} can only be different from zero in the presence of non-axial ligand-field components. In contrast to Kramers systems, there is no fundamental degeneracy in even-electron systems such as Ho^{III} if the ligand-field symmetry is low enough. In both compounds **1** and **2**, the dominant axial ligand-field contribution certainly comes from the central N atom (Supporting Information, Figure S3). However, also in both **1** and **2** the strict axiality is broken by the presence of weak low-symmetry components which originate from the six-fold negatively charged C_{80} cage and Sc ions with formal tripositive charge (Supporting Information, Figure S3). Such weak low-symmetry components are also found in other similar EMFs by single-crystal X-ray structure determination.[19] In contrast to **1**, the low-symmetry components directly affect the energy spectrum in **2** already at zero magnetic field and lead to a tunnel splitting between the two lowest-energy states. It is not an easy task to obtain a quantitative estimation of the influence of the non-axial ligand-field components on the tunnel splitting. From our observations, we derive that the direct effect of the non-axial components on

the tunnel splittings of the non-Kramers ion Ho^{III} is much stronger than the indirect effect in Dy^{III}, which requires the additional presence of internal magnetic fields. This reasoning is further supported by recent studies, which have shown that even in low-symmetry ligand fields Dy^{III} can possess a highly axial ground-state doublet.[17b,20]

Compound **2** adds to the list of lanthanide SIMs,[2] and it is the second example of an endohedral SIM. So far, only a few out of the large number of elemental combinations that form the endohedral unit have been identified as SMM. Further studies are needed to elucidate the static and dynamic magnetic properties of this fascinating new class of magnetic systems, which are expected to open doors to new applications. The metallofullerenes $Ho_2ScN@C_{80}$ and $Ho_3N@C_{80}$, which have not been studied here, can also be expected to exhibit interesting magnetic behavior. A weak intramolecular magnetic exchange coupling, similar as in the $Dy_xSc_{3-x}N@C_{80}$ series,[4] may be present, and detailed SQUID studies are planned.

In summary, we have demonstrated that $HoSc_2N@C_{80}$ exhibits strong magnetic anisotropy with a ground state characterized by a large angular momentum close to $m_{J,GS} = \pm 8$. Furthermore, $HoSc_2N@C_{80}$ is a field-induced SIM with relaxation times of up to several milliseconds at low temperatures. The large difference in magnetization relaxation times between $HoSc_2N@C_{80}$ and $DySc_2N@C_{80}$ is rationalized in that the low-symmetry ligand-field components introduced by the C_{80} cage must be more efficient by orders of magnitude in the case of $HoSc_2N@C_{80}$ than in $DySc_2N@C_{80}$.

Experimental Section

$HoSc_2N@C_{80}$ with I_h carbon cage isomer was synthesized by arc-discharge synthesis with NH_3 as a reactive gas atmosphere and separated from other Ho-Sc EMFs by recycling chromatography, as described in detail previously.[7] The magnetic properties were measured using a Quantum design MPMS-5XL SQUID magnetometer for fields of up to ± 50 kOe and temperatures from 1.85 to 6 K. Magnetic susceptibility was measured as $\chi = M/H$ at $H = 1$ kOe. The sample of **2** was prepared from toluene solution by drop-casting into half of a gelatine capsule. The diamagnetic background of the capsule was subtracted from the data. In the ac measurements, an oscillating field of amplitude $H_{ac} = 3.5$ Oe was employed. Further measurements with the sample frozen in 1-octadecene oil did not show any difference in the ac susceptibility. The dc measurements were not repeated with octadecene. The field-dependent magnetization was calculated by diagonalization of Equation (1) and the application of thermal statistics. Orientational averaging was performed by a 110-point Lebedev Laikov grid.[21] DFT calculations were performed using Firefly package[22] and B3LYP functional with def2-SVP basis set for carbon,[23] def2-TZVP for nitrogen,[23] and Stuttgart–Cologne effective core potentials for Sc (ECP10 MDF)[24] and Ho (4f-in-core ECP56 MWB-II)[25] with corresponding basis sets.

Acknowledgements

The authors acknowledge funding by the Swiss National Science Foundation (grants PZ00P2 142474, 200021–129861, and 200021–147143) and the Deutsche Forschungsgemeinschaft (projects PO 1602/1–1 and DU225/31–1 within the D–A–CH program).

Keywords: endohedral fullerenes · holmium · lanthanides · magnetic anisotropy · single-ion magnets

[1] a) S. Osa, T. Kido, N. Matsumoto, N. Re, A. Pochaba, J. Mrozinski, *J. Am. Chem. Soc.* **2004**, *126*, 420–421; b) V. Mereacre, A. M. Ako, R. Clérac, W. Wernsdorfer, I. J. Hewitt, C. E. Anson, A. K. Powell, *Chem. Eur. J.* **2008**, *14*, 3577–3584; c) R. Sessoli, A. K. Powell, *Coord. Chem. Rev.* **2009**, *253*, 2328; d) T. C. Stamatatos, S. J. Teat, W. Wernsdorfer, G. Christou, *Angew. Chem.* **2009**, *121*, 529–532; *Angew. Chem. Int. Ed.* **2009**, *48*, 521–524; e) L. Sorace, C. Benelli, D. Gatteschi, *Chem. Soc. Rev.* **2011**, *40*, 3092; f) J. D. Rinehart, J. R. Long, *Chem. Sci.* **2011**, *2*, 2078–2085; g) J. D. Rinehart, M. Fang, W. J. Evans, J. R. Long, *J. Am. Chem. Soc.* **2011**, *133*, 14236–14239; h) S. Demir, J. M. Zadrozny, M. Nippe, J. R. Long, *J. Am. Chem. Soc.* **2012**, *134*, 18546–18549; i) D. N. Woodruff, R. E. P. Winpenny, R. A. Layfield, *Chem. Rev.* **2013**, *113*, 5110–5148; j) F. Habib, M. Murugesu, *Chem. Soc. Rev.* **2013**, *42*, 3278–3288; k) M.-E. Boulon, G. Cucinotta, J. Luzon, C. Degl'Innocenti, M. Perfetti, K. Bernot, G. Calvez, A. Caneschi, R. Sessoli, *Angew. Chem.* **2013**, *125*, 368–372; *Angew. Chem. Int. Ed.* **2013**, *52*, 350–354; l) F. Habib, G. Brunet, V. Vieru, I. Korobkov, L. F. Chibotaru, M. Murugesu, *J. Am. Chem. Soc.* **2013**, *135*, 13242–13245; m) A. V. Funes, L. Carrella, E. Rentschler, P. Alborés, *Dalton Trans.* **2014**, *43*, 2361–2364.

[2] a) N. Ishikawa, M. Sugita, T. Ishikawa, S.-y. Koshihara, Y. Kaizu, *J. Am. Chem. Soc.* **2003**, *125*, 8694; b) M. A. AlDamen, J. M. Clemente-Juan, E. Coronado, C. Martí-Gastaldo, A. Gaita-Ariño, *J. Am. Chem. Soc.* **2008**, *130*, 8874–8875; c) M. A. AlDamen, S. Cardona-Serra, J. M. Clemente-Juan, E. Coronado, A. Gaita-Arino, C. Marti-Gastaldo, F. Luis, O. Montero, *Inorg. Chem.* **2009**, *48*, 3467; d) S.-D. Jiang, B.-W. Wang, G. Su, Z.-M. Wang, S. Gao, *Angew. Chem.* **2010**, *122*, 7610; *Angew. Chem. Int. Ed.* **2010**, *49*, 7448; e) M. Gonidec, E. S. Davies, J. McMaster, D. B. Amabilino, J. Veciana, *J. Am. Chem. Soc.* **2010**, *132*, 1756–1757; f) J. M. Zadrozny, J. R. Long, *J. Am. Chem. Soc.* **2011**, *133*, 20732; g) H. L. C. Feltham, Y. Lan, F. Klöwer, L. Ungur, L. F. Chibotaru, A. K. Powell, S. Brooker, *Chem. Eur. J.* **2011**, *17*, 4362–4365; h) S.-D. Jiang, B.-W. Wang, H.-L. Sun, Z.-M. Wang, S. Gao, *J. Am. Chem. Soc.* **2011**, *133*, 4730–4733; i) J.-L. Liu, Y.-C. Chen, Y.-Z. Zheng, W.-Q. Lin, L. Ungur, W. Wernsdorfer, L. F. Chibotaru, M.-L. Tong, *Chem. Sci.* **2013**, *4*, 3310–3316; j) C. R. Ganivet, B. Ballesteros, G. de La Torre, J. M. Clemente-Juan, E. Coronado, T. Torres, *Chem. Eur. J.* **2013**, *19*, 1457–1465; k) K. R. Meihaus, J. R. Long, *J. Am. Chem. Soc.* **2013**, *135*, 17952–17957; l) K. S. Pedersen, L. Ungur, M. Sigrist, A. Sundt, M. Schau-Magnussen, V. Vieru, H. Mutka, S. Rols, H. Weihe, O. Waldmann, *Chem. Sci.* **2014**, *5*, 1650–1660; m) E. Lucaccini, L. Sorace, M. Perfetti, J.-P. Costes, R. Sessoli, *Chem. Commun.* **2014**, *50*, 1648–1651.

[3] R. Westerström, J. Dreiser, C. Piamonteze, M. Muntwiler, S. Weyeneth, H. Brune, S. Rusponi, F. Nolting, A. Popov, S. Yang, L. Dunsch, T. Greber, *J. Am. Chem. Soc.* **2012**, *134*, 9840–9843.

[4] R. Westerström, J. Dreiser, C. Piamonteze, M. Muntwiler, S. Weyeneth, K. Krämer, S.-X. Liu, S. Decurtins, A. Popov, S. Yang, L. Dunsch, T. Greber, *Phys. Rev. B* **2014**, *89*, 060406.

[5] a) S. Stevenson, G. Rice, T. Glass, K. Harich, F. Cromer, M. R. Jordan, J. Craft, E. Hadju, R. Bible, M. M. Olmstead, K. Maitra, A. J. Fisher, A. L. Balch, H. C. Dorn, *Nature* **1999**, *401*, 55–57; b) L. Dunsch, M. Krause, J. Noack, P. Georgi, *J. Phys. Chem. Solids* **2004**, *65*, 309–315; c) L. Dunsch, S. Yang, *Phys. Chem. Chem. Phys.* **2007**, *9*, 3067–3081; d) A. A. Popov, S. Yang, L. Dunsch, *Chem. Rev.* **2013**, *113*, 5989–6113.

[6] V. Vieru, L. Ungur, L. F. Chibotaru, *J. Phys. Chem. Lett.* **2013**, *4*, 3565–3569.

[7] Y. Zhang, A. A. Popov, S. Schiemenz, L. Dunsch, *Chem. Eur. J.* **2012**, *18*, 9691–9698.

[8] A. A. Popov, L. Dunsch, *J. Am. Chem. Soc.* **2008**, *130*, 17726–17742.

[9] a) A. Abragam and B. Bleaney in *Electron paramagnetic resonance in transition ions*, Clarendon, Oxford, **1970**; b) L. F. Chibotaru, L. Ungur, *J. Chem. Phys.* **2012**, *137*, 064112.

[10] J. S. Griffith, *Phys. Rev.* **1963**, *132*, 316–319.

[11] a) M. Wolf, K.-H. Müller, D. Eckert, Y. Skourski, P. Georgi, R. Marczak, M. Krause, L. Dunsch, *J. Magn. Magn. Mater.* **2005**, *290–291*, 290–293; b) M. Wolf, K.-H. Müller, Y. Skourski, D. Eckert, P. Georgi, M. Krause, L. Dunsch, *Angew. Chem.* **2005**, *117*, 3371–3374; *Angew. Chem. Int. Ed.* **2005**, *44*, 3306–3309.

[12] J. Dreiser, K. S. Pedersen, C. Piamonteze, S. Rusponi, Z. Salman, M. E. Ali, M. Schau-Magnussen, C. A. Thuesen, S. Piligkos, H. Weihe, H. Mutka, O. Waldmann, P. Oppeneer, J. Bendix, F. Nolting, H. Brune, *Chem. Sci.* **2012**, *3*, 1024–1032 and discussion in the Supporting Information.

[13] a) H. B. G. Casimir, F. K. du Pré, *Physica* **1938**, *5*, 507–511; b) K. S. Cole, R. H. Cole, *J. Chem. Phys.* **1941**, *9*, 341–351.

[14] a) R. Orbach, *Proc. R. Soc. London Ser. A* **1961**, *264*, 458–484; b) M. B. Walker, *Can. J. Phys.* **1968**, *46*, 1347–1353; c) A. Singh, K. N. Shrivastava, *Phys. Status Solidi B* **1979**, *95*, 273–277; d) K. N. Shrivastava, *Phys. Status Solidi B* **1983**, *117*, 437–458.

[15] J. M. Zadrozny, M. Atanasov, A. M. Bryan, C.-Y. Lin, B. D. Rekken, P. P. Power, F. Neese, J. R. Long, *Chem. Sci.* **2013**, *4*, 125–138.

[16] a) A. Uldry, F. Vernay, B. Delley, *Phys. Rev. B* **2012**, *85*, 125133; b) Y. Zhang, D. Krylov, S. Schiemenz, M. Rosenkranz, R. Westerström, J. Dreiser, T. Greber, B. Büchner, A. A. Popov, *Nanoscale* **2014**, DOI: 10.1039/C4NR02864C.

[17] a) J. J. Baldoví, J. J. Borrás-Almenar, J. M. Clemente-Juan, E. Coronado, A. Gaita-Ariño, *Dalton Trans.* **2012**, *41*, 13705–13710; b) N. F. Chilton, D. Collison, E. J. L. McInnes, R. E. P. Winpenny, A. Soncini, *Nat. Commun.* **2013**, *4*, 2551.

[18] a) N. Ishikawa, M. Sugita, T. Okubo, N. Tanaka, T. Iino, Y. Kaizu, *Inorg. Chem.* **2003**, *42*, 2440–2446; b) N. Ishikawa, M. Sugita, W. Wernsdorfer, *Angew. Chem.* **2005**, *117*, 2991–2995; *Angew. Chem. Int. Ed.* **2005**, *44*, 2931–2935; c) N. Ishikawa, M. Sugita, W. Wernsdorfer, *J. Am. Chem. Soc.* **2005**, *127*, 3650–3651.

[19] a) M. M. Olmstead, A. de Bettencourt-Dias, J. C. Duchamp, S. Stevenson, H. C. Dorn, A. L. Balch, *J. Am. Chem. Soc.* **2000**, *122*, 12220–12226; b) S. Stevenson, C. J. Chancellor, H. M. Lee, M. M. Olmstead, A. L. Balch, *Inorg. Chem.* **2008**, *47*, 1420–1427.

[20] K. Bernot, J. Luzon, L. Bogani, M. Etienne, C. Sangregorio, M. Shanmugam, A. Caneschi, R. Sessoli, D. Gatteschi, *J. Am. Chem. Soc.* **2009**, *131*, 5573–5579.

[21] V. I. Lebedev, D. N. Laikov, *Dokl. Akad. Nauk* **1999**, *366*, 741–745.

[22] A. A. Granovsky, Firefly version 8.0.0, http://classic.chem.msu.su/gran/firefly/index.html

[23] F. Weigend, R. Ahlrichs, *Phys. Chem. Chem. Phys.* **2005**, *7*, 3297–3305.

[24] M. Dolg, U. Wedig, H. Stoll, H. Preuss, *J. Chem. Phys.* **1987**, *86*, 866–872.

[25] M. Dolg, H. Stoll, A. Savin, H. Preuss, *Theor. Chim. Acta* **1989**, *75*, 173–194.

Received: April 11, 2014
Revised: June 11, 2014
Published online on August 27, 2014